Infinite Wavelength Resonant Antennas With Monopolar Radiation Pattern Based on Periodic Structures

Anthony Lai, *Student Member, IEEE*, Kevin M. K. H. Leong, *Member, IEEE*, and Tatsuo Itoh, *Fellow, IEEE*

Abstract—The analysis of resonant-type antennas based on the fundamental infinite wavelength supported by certain periodic structures is presented. Since the phase shift is zero for a unit-cell that supports an infinite wavelength, the physical size of the antenna can be arbitrary; the antenna's size is independent of the resonance phenomenon. The antenna's operational frequency depends only on its unit-cell and the antenna's physical size depends on the number of unit-cells. In particular, the unit-cell is based on the composite right/left-handed (CRLH) metamaterial transmission line (TL). It is shown that the CRLH TL is a general model for the required unit-cell, which includes a nonessential series capacitance for the generation of an infinite wavelength. The analysis and design of the required unit-cell is discussed based upon field distributions and dispersion diagrams. It is also shown that the supported infinite wavelength can be used to generate a monopolar radiation pattern. Infinite wavelength resonant antennas are realized with different number of unit-cells to demonstrate the infinite wavelength resonance.

Index Terms—Metamaterials, microstrip antennas, periodic structures.

I. INTRODUCTION

RECENTLY, research into metamaterials based on periodic unit-cells for microwave applications has grown rapidly with the verification of left-handed (LH) metamaterials [1], [2]. In particular, the transmission line approach of LH metamaterials has led to the realization of the composite right/left-handed (CRLH) transmission line (TL) which includes LH and right-handed (RH) attributes [3]. The CRLH TL has many unique properties such as supporting a fundamental backward wave (anti-parallel group and phase velocities) and zero propagation constant ($\beta = 0$) with zero or non-zero group velocity at a discrete frequency. The backward wave property of the CRLH TL and other LH-based TLs has been used to realize novel, small *half-wavelength* resonant antennas [4], [5]. The infinite wavelength property ($\beta = 0$, $\omega \neq 0$) of the CRLH TL has been used to realize several size-independent resonant structures such as the zeroth order resonator [6] and infinite wavelength series divider [7].

In this paper, the analysis and design of resonant, planar antennas based on the fundamental infinite wavelength property of the CRLH TL is presented. Since an infinite wavelength oc-

curs when the propagation constant is zero, the frequency of the proposed antenna does not depend on its physical length, but only on the reactance provided by its unit-cell. Therefore, the physical size of the proposed antenna can be arbitrary; this is useful to realize electrically small or electrically large antennas. By properly designing the unit-cell, the radiation pattern of the antenna at the infinite wavelength frequency can also be tailored. In particular, it is shown that the CRLH TL unit-cell is the general model for the required unit-cell which consists of a series capacitance, a series inductance, a shunt capacitance, and a shunt inductance. The CRLH TL unit-cell's shunt resonance determines the infinite wavelength frequency and thus the antenna's operational frequency. As a result, a CRLH TL unit-cell without series capacitance referred to as an inductor-loaded TL unit-cell can also be used to realize the antenna. By modifying the equivalent shunt capacitance and/or shunt inductance circuit parameters of the unit-cell, the operational frequency and the physical size of the realized antennas can be controlled. Furthermore, the unique "equal amplitude/phase" electric-field distribution of an infinite wavelength excited on the antenna gives rise to a monopolar radiation pattern.

The proposed periodic design methodology offers a straightforward design approach based on the characteristics of a single unit-cell. Based on this periodic structure methodology, CRLH antennas with monopolar radiation patterns consisting of two, four, and six unit-cells are numerically and experimentally verified. Inductor-loaded antennas with monopolar radiation patterns consisting of two, four, and six unit-cells are also investigated. The input impedance, gain, and radiation pattern as a function of the number of unit-cells are examined for both types of antennas. The effect of adding unit-cells in the non-resonant dimension of the proposed antenna is also investigated. In addition, the choice of CRLH unit-cell or inductor-loaded unit-cell for dual-mode antenna configurations is discussed.

II. THEORY

Since the proposed infinite wavelength antenna is based on a periodic design approach, a unit-cell capable of supporting an infinite wavelength is discussed in Section II-A. In addition, the monopolar radiation pattern of the proposed infinite wavelength antenna is presented.

A. Fundamental Infinite Wavelength Unit-Cell

To realize a resonant-type planar antenna with no dependence on its physical size, a TL structure that supports an infinite wavelength at its fundamental mode is required. A practical realiza-
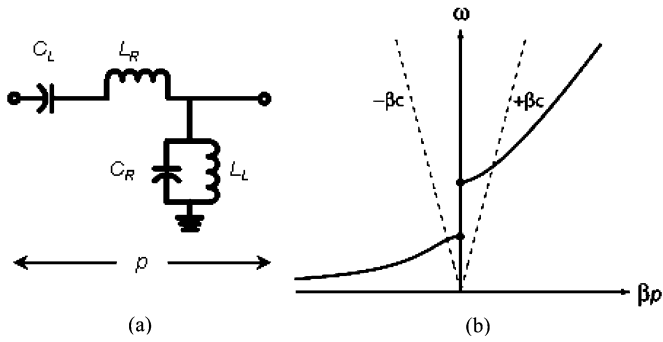
Fig. 1. CRLH TL. (a) LC unit-cell of length p. (b) Dispersion diagram showing fundamental LH mode and RH mode.

Fig. 2. Four-cell open-ended resonators. (a) CRLH TL unit-cell. (b) No series components.

tion of a LH TL, which includes unavoidable RH effects, known as a CRLH TL is able to support an infinite wavelength ($\beta = 0$ when $\omega \neq 0$) and therefore can be used to realize the proposed antenna.

The equivalent circuit model of the CRLH TL unit-cell is shown in Fig. 1(a). By applying periodic boundary conditions (PBCs) related to the Bloch-Floquet theorem, the CRLH TL unit-cell's dispersion relation is determined to be

$$\beta(\omega) = \frac{1}{p}\cos^{-1}\left(1 - \frac{1}{2}\left(\frac{\omega_L^2}{\omega^2} + \frac{\omega^2}{\omega_R^2} - \frac{\omega_L^2}{\omega_{\mathrm{se}}^2} - \frac{\omega_L^2}{\omega_{\mathrm{sh}}^2}\right)\right). \quad (1)$$

where

$$\omega_L = \frac{1}{\sqrt{C_L L_L}}, \quad \omega_R = \frac{1}{\sqrt{C_R L_R}}$$
$$\omega_{\mathrm{se}} = \frac{1}{\sqrt{C_L L_R}}, \quad \omega_{\mathrm{sh}} = \frac{1}{\sqrt{C_R L_L}}. \quad (2)$$

The dispersion diagram of the CRLH TL unit-cell is shown in Fig. 1(b). The CRLH TL supports a fundamental LH wave (phase advance) at lower frequencies and a RH wave (phase delay) at higher frequencies.

In general, the series resonance (ω_{se}) and the shunt resonance ω_{sh}) are not equal and two non-zero frequency points with $\beta = 0$ are present. These two points are referred to as infinite wavelength points and are determined by the series resonance and shunt resonance of the unit-cell as given in (2). By cascading a CRLH TL unit-cell of length p, N times, a CRLH TL of length $L = N * p$ can be realized. The CRLH TL can be used as a resonator under the resonance condition

$$\beta_n = \frac{n\pi}{L} \quad (3)$$

where n is the resonance mode number and can be a positive or negative integer and even zero [6]. In the case where $n = 0$, an infinite wavelength is supported and the resonance condition is independent of the CRLH TL's length (i.e., number of unit-cells, N, can be arbitrary). In the case of open boundary conditions, the infinite wavelength frequency is determined by the shunt resonance frequency, ω_{sh} which is given by

$$\omega_{\mathrm{sh}} = \frac{1}{\sqrt{C_R L_L}}. \quad (4)$$

Fig. 3. Resonance peaks of open-ended resonators shown in Fig. 2.

Since only the CRLH TL unit-cell's shunt resonance determines the infinite wavelength frequency, the series components have no effect. As an example, consider the open-ended resonator based on four CRLH unit-cells as shown in Fig. 2(a) with $C_L = 1.50$ pF, $L_R = 1.00$ pF, $C_R = 1.45$ pF, and $L_L = 1.95$ nH, which corresponds to $f_{\mathrm{sh}} = 3.0$ GHz. The open-ended resonator is coupled to the input/output port with capacitors of $C_c = 0.01$ pF. An open-ended resonator with the series components eliminated is shown in Fig. 2(b).

The resonance peaks of the two open-ended resonators are displayed in Fig. 3 and demonstrate that only the shunt components determine the infinite wavelength resonance in the case of open boundary conditions. Therefore, an inductor-loaded TL unit-cell with the same shunt components as the CRLH TL unit-cell has the same infinite wavelength frequency as the CRLH TL unit-cell. The unit-cell of the inductor-loaded TL is shown in Fig. 4(a) and its propagation constant is given by

$$\beta(\omega) = \frac{1}{p}\cos^{-1}\left(1 + \frac{1}{2}\left(\frac{L_R}{L_L} - \frac{\omega^2}{\omega_R^2}\right)\right). \quad (5)$$

The dispersion diagram of the inductor-loaded TL is plotted in Fig. 4(b).

The inductor-loaded TL has a DC-offset just like the CRLH TL, but the dispersion characteristics are quite different; phase advance or phase delay can occur for the CRLH TL, while only
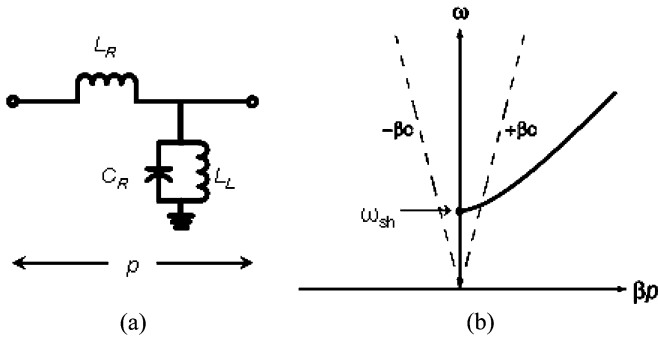
Fig. 4. Inductor-loaded TL. (a) LC unit-cell of length p. (b) Dispersion diagram.

Fig. 5. Microstrip patch antennas with dimensions $p \times p\ \mathrm{mm}^2$; resonant length along y-direction. (a) Conventional supporting half-wavelength. (b) CRLH supporting infinite wavelength.

phase delay can occur for the inductor-loaded TL. Since the resonance condition of (3) is independent of the CRLH TL's or inductor-loaded TL's length at the infinite wavelength frequency, the open-ended resonators of Fig. 2 can be used to realize size independent resonant antennas. Although the number of unit-cells used to realize an infinite wavelength resonator has no effect on its operational frequency, the input impedance of the structure is dependent on the number of unit-cells and is given by

$$Z_{\mathrm{in}} = -jZ_0 \cot(\beta l) \overset{b \to 0}{\approx} \frac{1}{NY} \qquad (6)$$

where Y is the admittance of the unit-cell [6], given by $Y = j(\omega C_R - 1/(\omega L_L))$.

B. Infinite Wavelength Antennas With Monopolar Radiation

By using an open-ended resonator that supports an infinite wavelength, an infinite wavelength resonant antenna with an operational frequency independent of its physical size can be realized. Such an antenna can be made electrically large or small, the latter of which was demonstrated in [8] with a patch-like pattern. In contrast to [8], electrically large and small infinite wavelength antennas with monopolar radiation patterns are demonstrated. Various low-profile monopolar antennas have been realized [9]–[13] based on reactive loading with shorting pins. However, the placement and number of shorting pins for these monopolar antennas were strictly based on numerical studies. In order to discuss the radiation mechanism behind the proposed antenna, first consider the conventional microstrip patch antenna as shown in Fig. 5(a). The patch antenna can be modeled as a square cavity with perfect magnetic conductor (PMC) walls. At its fundamental mode, the patch antenna supports a half-wavelength along its resonant length. Therefore, the non-zero equivalent magnetic current density at each radiating edge is given by

$$\overrightarrow{M_S} = -2\hat{n} \times \overrightarrow{E} \qquad (7)$$

where $\hat{n}$ is the unit normal to the edge, $\overrightarrow{E}$ is the electric field at the edge, and the factor of 2 is due to the ground plane [14]. It is the two equivalent magnetic current densities at the radiating edges of the patch antenna that contribute to its radiation pattern. Next consider the proposed CRLH antenna shown in Fig. 5(b). Since the CRLH TL can support an infinite wavelength, the field distributions along the perimeter of the CRLH
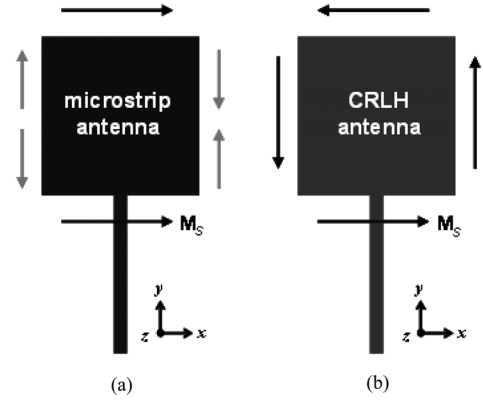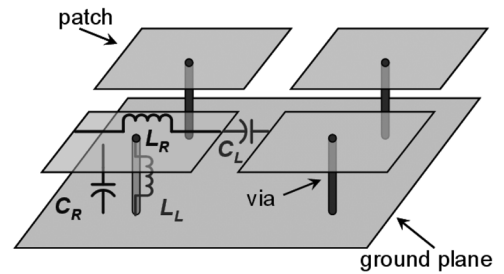
Fig. 6. Microstrip realization of a CRLH TL based on Sievenpiper high impedance surface.

antenna are in-phase when operated at its infinite wavelength frequency. Therefore, the equivalent magnetic current densities at the edges described by (7) form a loop as shown in Fig. 5(b). It is this equivalent magnetic loop that produces the monopolar radiation pattern; a magnetic loop is an ideal electric dipole by duality. As a result, the proposed infinite wavelength antennas are polarized in the theta-direction.

III. CRLH TL UNIT-CELL REALIZATION

As mentioned in Section II, the CRLH TL unit-cell is the general model for the monopolar unit-cell. To realize the required capacitances and inductances of the CRLH TL unit-cell model, a physical implementation has to be chosen. Lumped components or distributed structures can be used, but for radiation-type applications purely lumped component-based structures are impractical due to their inability to radiate. Due to the popularity of microstrip technology for planar antennas, the CRLH TL unit-cell is based on microstrip. One structure that is commonly used to realize a CRLH TL is the Sievenpiper mushroom structure [15], [16] as shown in Fig. 6.

The mushroom unit-cell consists of a square metallic via connected to the ground plane by a shorting post. The mushroom's LH capacitance (C_L) is attributed to the edge coupling between the unit-cells and the mushroom's LH inductance (L_L) is due to the shorting post to ground. The RH effects are due to the capacitive coupling (C_R) between the patch and ground plane and the current flow atop the patch (L_R). By changing the physical properties of the mushroom unit-cell (e.g., patch size, shorting post radius, dielectric constant, etc.), the equivalent

capacitances and inductances can be controlled. When there is no gap between the mushroom unit-cells, it simply becomes an inductor-loaded TL. The interdigital-based CRLH TL unit-cell discussed in [3] is another microstrip implementation of the CRLH TL unit-cell used for one-dimensional LH applications [17]. The choice of the mushroom unit-cell over the interdigital-based unit-cell is for radiation pattern preference. In the case of the mushroom unit-cell, symmetrical boundary conditions similar to the center-shorted microstrip patch antenna exist and a monopolar radiation pattern is possible. In the case of the interdigital-based unit-cell antenna implemented in [8], a patch-like radiation is present since there is only one radiating open-boundary.

IV. INFINITE WAVELENGTH RESONANT ANTENNA REALIZATION

In this section, several infinite wavelength antennas with monopolar radiation patterns are realized. The unit-cells for the proposed antennas are based on a modified mushroom unit-cell; the metallic patch does not need to be a square, but can be rectangular. The size of the patch, the dielectric constant, the period of the unit-cell, and the radius of the shorting post are all factors that control the dispersion curve of the unit-cell and in effect the resonant frequencies of the antenna [18]. A CRLH TL unit-cell and an inductor-loaded TL unit-cell are used to realize the infinite wavelength antennas. Both types of unit-cells have similar shunt reactance which means their infinite wavelength frequency will be similar. To demonstrate this effect, antennas consisting of two, four, and six CRLH TL unit-cells and two, four, and six inductor-loaded TL unit-cells are realized. In Section IV-A, the dimensions of the proposed unit-cells, the antenna's input impedance as a function of the number of unit-cells, and the radiation pattern/gain of the antennas are presented.

A. Proposed Antenna Design

The general model of the CRLH TL and the inductor-loaded TL based infinite wavelength antennas are shown in Fig. 7(a) and (b), respectively. Both figures show that proximity coupling is used as the feed network for the antennas. However, the feeding method varies depending on the number of unit-cells (N) as discussed below. All the antennas are realized on Rogers RT/Duroid 5880 with dielectric constant $\varepsilon_r = 2.2$ and thickness $h = 1.57$ mm. The CRLH TL unit-cell measures 7.3×15 mm^2 with a period of 7.5 mm, while the inductor loaded TL unit-cell measures 7.5×15 mm^2 with a period of 7.5 mm. The radius of the shorting post is 0.12 mm for both unit-cells and the shorting post is located at unit-cell's geometrical center. Therefore, the infinite wavelength frequencies for these unit-cells are very similar.

The calculated dispersion diagrams for each unit-cell are shown in Fig. 8 along with experimental resonant peaks of a five unit-cell open-ended resonator implementation. The infinite wavelength frequency for the CRLH TL unit-cell is 3.65 GHz and is 3.52 GHz for the inductor-loaded TL unit-cell as predicted by applying periodic boundary conditions on a single unit-cell. In contrast, the five unit-cell resonator implementation predicts an infinite wavelength frequency of
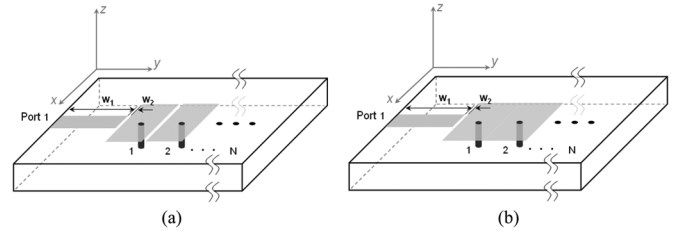
Fig. 7. Model of antennas composed of N unit-cells. (a) CRLH TL unit-cell implementation. (b) Inductor-loaded TL unit-cell implementation.
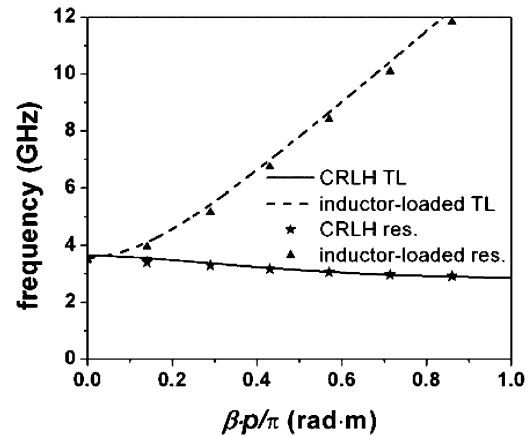
Fig. 8. Dispersion diagram of CRLH and inductor-loaded unit-cell of Fig. 7.

3.51 GHz and 3.50 GHz for the CRLH TL unit-cell and for the inductor-loaded TL unit-cell, respectively. The infinite wavelength frequency of the unit-cell can be controlled by changing the substrate or unit-cell parameters. With reference to the infinite wavelength frequency relation of (4), increasing the patch area and/or substrate permittivity will increase the RH capacitance (C_R), while decreasing the radius of the shorting post will increase the LH inductance (L_L). These effects will lower the infinite wavelength frequency. Increasing or decreasing the substrate height will have little effect on the infinite wavelength frequency since C_R is inversely proportional and L_L is proportional to substrate height. In addition, the substrate and unit-cell parameters will also affect the overall antenna's bandwidth and efficiency performance. To enhance bandwidth, the substrate height should relatively thick while the substrate permittivity should be low [13]. In order to enhance the efficiency of the antenna, the substrate loss tangent should be low and the shorting post radius should be increased. As a result, a tradeoff between antenna bandwidth/efficiency and the antenna size has to be considered.

B. Input Impedance

The input impedance $(Z_{\text{in}} = R + jX \, \Omega)$ of each antenna implementation is computed using Ansoft HFSS v10. A 50 Ω line was directly attached to the input edge of each antenna and deembedded to calculate the input impedance. The real part and imaginary component of the input impedance for the CRLH TL based antennas are shown in Fig. 9(a) and (b), respectively. The real part and imaginary component of the input impedance for the inductor-loaded TL based antennas are shown in Fig. 10(a) and (b), respectively. In the case of

TABLE I
SUMMARY OF INPUT IMPEDANCE AND CORRESPONDING RESONANT FREQUENCY OF PROPOSED ANTENNAS

	frequency	$Z_{in}=R+jX$ (Ω)
2 cells (CRLH)	3.47 GHz	1060.1+j0.0
4 cells (CRLH)	3.53 GHz	410.0-j15.0
6 cells (CRLH)	3.55 GHz	253.0-j73.0
2 cells (inductor-loaded)	3.44 GHz	890.0+j0.0
4 cells (inductor-loaded)	3.51 GHz	310.0+j20.6
6 cells (inductor-loaded)	3.53 GHz	178.8+j41.0
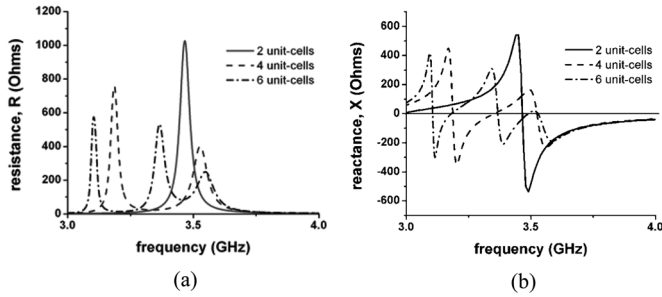
Fig. 9.   CRLH antenna input impedance. (a) Real part (R). (b) Imaginary part (X).
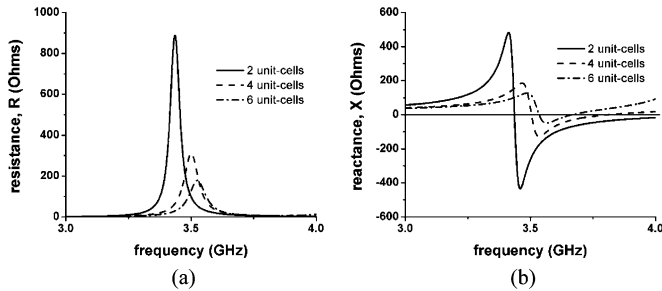
Fig. 10.   CRLH antenna input impedance. (a) Real part (R). (b) Imaginary part (X).

Fig. 11.   Experimental return loss of the CRLH and inductor-loaded two unit-cell antennas.

the CRLH TL based antennas, other resonant modes below the $n = 0$ mode are present as observed in Fig. 9. However, for the generation of the monopolar pattern and for size independence, only the $n = 0$ mode is desired. The $n = 0$ mode is the lowest mode for the inductor-loaded TL based antennas because the inductor-loaded TL does not support a backward wave unlike the CRLH TL.

The resonant frequency of the proposed antennas is defined as the frequency where the real part of the impedance reaches a maximum, independent of the value of reactance [19], which is close to zero. The input impedance and corresponding infinite wavelength resonant frequency obtained from HFSS for the antennas are summarized in Table I. From Table I, it can be observed that the infinite wavelength frequency increases slightly as the number of unit-cells increases. As the number of unit-cells increases, the infinite wavelength frequency approaches the value predicted by applying PBCs on a single unit-cell. Although the inductor-loaded antennas do not have series capacitance, their infinite wavelength frequency is very similar to the
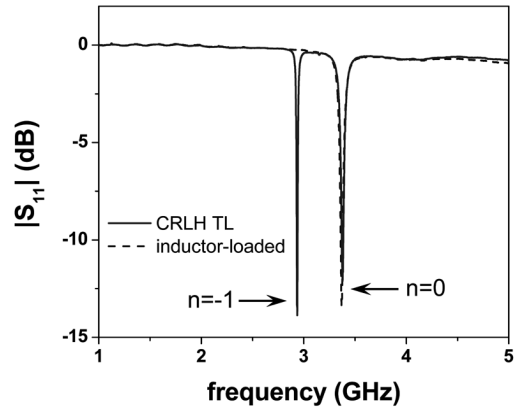
CRLH antennas. In addition, the input impedance follows the trend predicted by (6); the input impedance decreases as the number of unit-cells increases. Also, the CRLH based antenna's input reactance becomes capacitive as more unit-cells are added, while the inductor-loaded antenna's input reactance becomes inductive as more unit-cells are added.

C. Two Unit-Cell Antenna Realization

The input impedance for both the CRLH and inductor-loaded two unit-cell antennas is quite high for quarter wavelength matching. Therefore, proximity coupling is used to match both antennas to a 50 Ω line as shown in Fig. 7 with $w_1 = 15.0$ mm and $w_2 = 0.2$ mm. The experimental return loss of the CRLH and inductor-loaded two unit-cell antenna are shown in Fig. 11. For the CRLH based antenna, a return loss of -12.34 dB is obtained at $f_0 = 3.38$ GHz, while a return loss of -13.91 dB at $f_0 = 3.37$ GHz is obtained for the inductor-loaded antenna. The electrical size of the antennas is $\lambda_o/6 \times \lambda_o/6 \times \lambda_o/57$ at f_0. These results show that the two unit-cell antenna is not matched exactly at the predicted infinite wavelength frequency of Table I. This is due to the high input resistance of the antenna.

The electric-field distribution underneath the two unit-cell CRLH antenna for the $n = -1$ $(\beta = -180°)$ and $n = 0$ mode are shown in Fig. 12(a) and (b), respectively. Ansoft HFSS was used to obtain these field plots. The $n = -1$ mode distribution shows that the electric-field is $180°$ out-of-phase corresponding to a half-wavelength. As a result, the equivalent magnetic current densities along the perimeter of the antenna for the $n = -1$
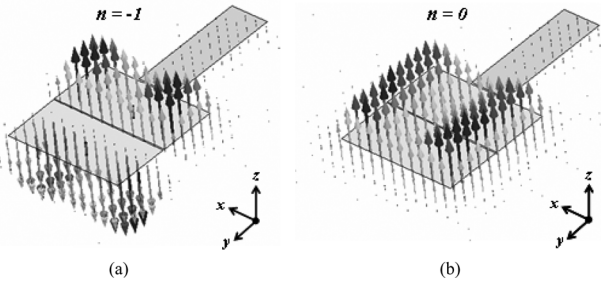
Fig. 12. Electric-field distribution underneath two unit-cell CRLH antenna obtained via Ansoft HFSS. (a) Half-wavelength, $n = -1$ mode. (b) Infinite wavelength, $n = 0$ mode.

mode form a distribution comparable to Fig. 5(a) and the radiation pattern will be similar to a conventional patch antenna. The $n = 0$ distribution shows that the electric-field is in-phase verifying that an infinite wavelength is supported. Therefore, the equivalent magnetic current densities along the perimeter of the antenna for the $n = 0$ mode form a loop comparable to Fig. 5(b) and a monopolar radiation occurs. Since the field distribution for the $n = 0$ mode does not change much within the bandwidth ($< 1\%$) the monopolar radiation is maintained over the bandwidth. By using the $n = -1$ and $n = 0$ mode, the proposed antennas can be used in dual-mode applications as discussed in [18].

The field distribution of the infinite wavelength antenna shown in Fig. 12(b) is similar to the TM_{01} mode of a conventional circular patch antenna. However, the TM_{01} mode is a higher order mode which makes the conventional circular patch antenna impractical for compact wireless devices. By placing a shorting post at the center of the conventional circular patch antenna, the TM_{01} becomes the fundamental mode as discussed in [20]. It was demonstrated in [21] that a mode similar to the circular patch's TM_{01} mode can be excited in non-circular patches shorted in the center to produce a fundamental monopolar radiation pattern. The resulting radiation patterns of the proposed antenna are similar to a top-loaded monopole [22], [23], but with the added benefit that the antenna size/gain is independent of the resonant frequency. As a result, the gain of the proposed antennas can be increased by adding unit-cells in the plane of the antenna, while the only way to increase the gain of a top-loaded monopole is by using an array of top-loaded monopoles.

The numerical and experimental radiation patterns of the CRLH and inductor-loaded antennas shown respectively in Figs. 13 and 14 reveal the expected monopolar radiation pattern. A maximum gain of 0.87 dBi and 0.70 dBi is experimentally obtained for the CRLH TL based antenna and for the inductor-loaded TL based antenna, respectively. In addition, the x-y plane radiation pattern and cross-polarization (normalized relative to co-polarization) of the CRLH antenna are shown in Fig. 13(c) and (d), respectively. Fig. 13(c) illustrates the omnidirectional coverage in the x-y plane provided by the monopolar antenna, while Fig. 13(d) shows that the cross-polarization is less than the co-polarization. The inductor-loaded antenna has similar x-y plane and cross-polarization patterns.
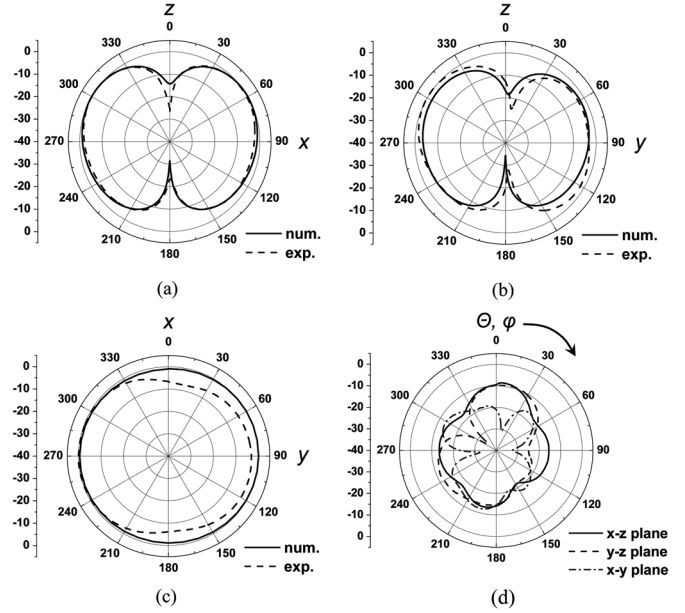
Fig. 13. Two unit-cell CRLH antenna radiation patterns. (a) Phi $= 0°$ (x-z plane). (b) Phi $= 90°$ (y-z plane). (c) Theta $= 90°$ (x-y plane). (d) Experimental cross-polarizations normalized to co-polarizations.
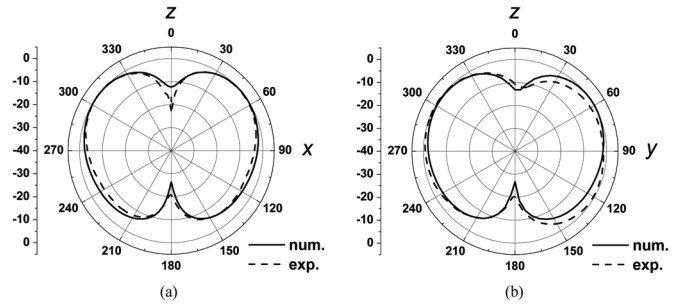
Fig. 14. Two unit-cell inductor-loaded antenna radiation patterns. (a) Phi $= 0°$ (x-z plane). (b) Phi $= 90°$ (y-z plane).

These patterns verify that the antennas are polarized in the theta-direction as discussed in Section II-B.

D. Effect of Increasing the Number of Unit-Cells

Additional unit-cells are added along the y-direction to create four and six unit-cell antennas as depicted in Fig. 7. A single section quarter wavelength transformer is used to match each four and six unit-cell antenna to a 50 Ω line. Only the real part of the input impedance shown in Table I is considered in the matching. The experimental infinite wavelength frequency, return loss, peak gain, and radiation efficiency using the Wheeler cap method [24] of the two, four, and six unit-cell antennas are displayed in Table II. The electrical size of the four unit-cell antennas is $\lambda_o/6 \times \lambda_o/3 \times \lambda_o/53$ at f_0 and the electrical size of the six unit-cell antennas is $\lambda_o/6 \times \lambda_o/2 \times \lambda_o/53$ at f_0. Although the antennas become physically larger, the infinite wavelength frequency remains approximately constant. In addition, gain increases as the antenna becomes physically larger. The radiation efficiency of the two unit-cell antennas is smaller than the four

TABLE II
EXPERIMENTAL RESULTS FOR TWO, FOUR, AND SIX UNIT-CELL ANTENNAS

	frequency	return loss	peak gain	rad. efficiency
2 cells (CRLH)	3.38 GHz	-12.34 dB	0.87 dBi	70%
4 cells (CRLH)	3.52 GHz	-17.33 dB	4.50 dBi	88%
6 cells (CRLH)	3.55 GHz	-11.17 dB	5.17 dBi	91%
2 cells (inductor-loaded)	3.37 GHz	-13.91 dB	0.70 dBi	69%
4 cells (inductor-loaded)	3.49 GHz	-20.50 dB	4.17 dBi	91%
6 cells (inductor-loaded)	3.53 GHz	-35.02 dB	5.00 dBi	90%
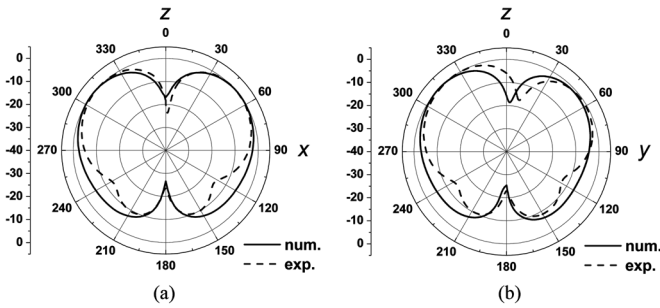
Fig. 15. Four unit-cell CRLH antenna radiation patterns. (a) $\mathrm{Phi} = 0°$ (x-z plane). (b) $\mathrm{Phi} = 90°$ (y-z plane).
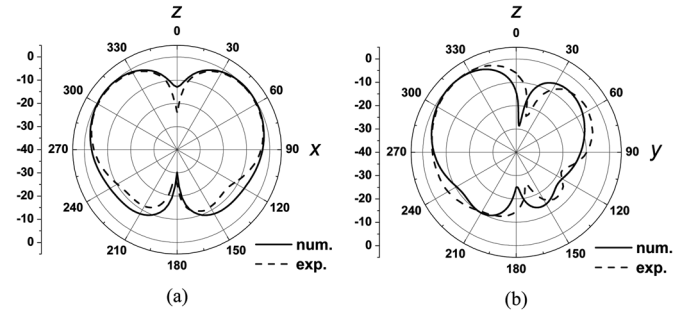
Fig. 17. Six unit-cell CRLH antenna radiation patterns. (a) $\mathrm{Phi} = 0°$ (x-z plane). (b) $\mathrm{Phi} = 90°$ (y-z plane).
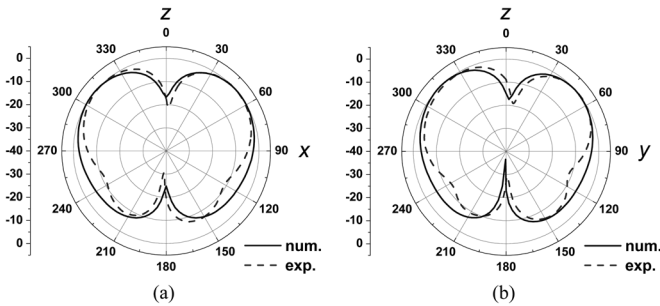
Fig. 16. Four unit-cell inductor-loaded antenna radiation patterns. (a) $\mathrm{Phi} = 0°$ (x-z plane). (b) $\mathrm{Phi} = 90°$ (y-z plane).
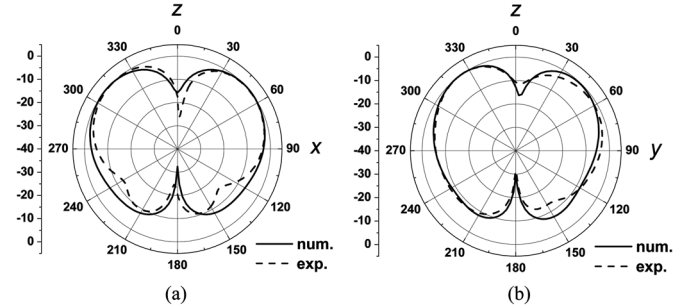
Fig. 18. Six unit-cell inductor-loaded antenna radiation patterns. (a) $\mathrm{Phi} = 0°$ (x-z plane).(b) $\mathrm{Phi} = 90°$ (y-z plane).

and six unit-cell antennas because of operation away from resonance. The x-y plane and cross-polarization of the four and six unit-cell CRLH antennas are similar to those of the two unit-cell CRLH antenna and therefore are not shown.

The predicted infinite wavelength frequencies of Table I show good agreement with the measured infinite wavelength frequencies of Table II. The numerical and experimental radiation patterns for the CRLH and inductor-loaded four unit-cell antennas are shown in Figs. 15 and 16, respectively. While, the numerical and experimental radiation patterns for the CRLH and inductor-loaded six unit-cell antennas are shown in Figs. 17 and 18, respectively. The expected monopolar pattern is obtained. However, the pattern is asymmetrical in the y-z plane. This can be attributed to the feed and that the antenna is operated in the fast-wave region [25] as seen in Figs. 1(b) and 4(b), which means that the unit-cell is inherently radiative. This asymmetry can be eliminated by using a coaxial feed at the center of the antenna.

E. Effect of Increasing Unit-Cells in Non-Resonant Direction

The previous sections showed the effect of adding unit-cells along the resonant length of the antenna. In this section, it is shown that unit-cells can be added to the non-resonant direction of the antenna to increase gain and to avoid the asymmetrical radiation pattern present in the six unit-cell antenna realizations with an edge feed. The proposed antenna is depicted in Fig. 19, which consists of four inductor-loaded unit-cells in the y-direction and two inductor-loaded unit-cells in the x-direction forming a square antenna aperture. The inductor-loaded unit-cells are the same as the ones used to realize the antennas presented in Sections IV-C and D

The feed used for the two unit-cell antennas is slightly modified in order to excite the entire structure. The numerical and experimental return loss of the enlarged antenna is shown in Fig. 20(a) along with the experimental return loss of the original two unit-cell inductor-loaded antenna for comparison. An experimental return loss of -6.4 dB is obtained at $f_0 = 3.58$ GHz;
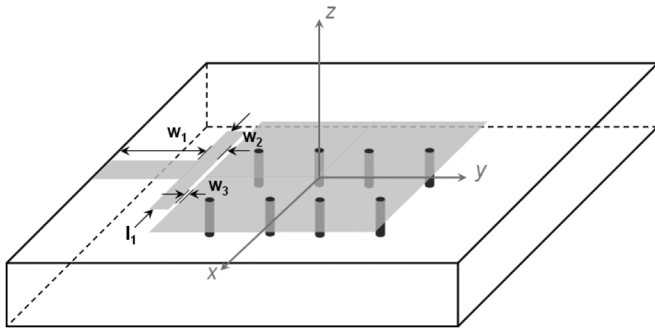
Fig. 19. Enlarged aperture monopolar antenna based on antenna of Fig. 7(b); $w_1 = 15.0\,\text{mm}$, $w_2 = 2.0\,\text{mm}$, $w_3 = 0.2\,\text{mm}$, $l_1 = 26.0\,\text{mm}$.
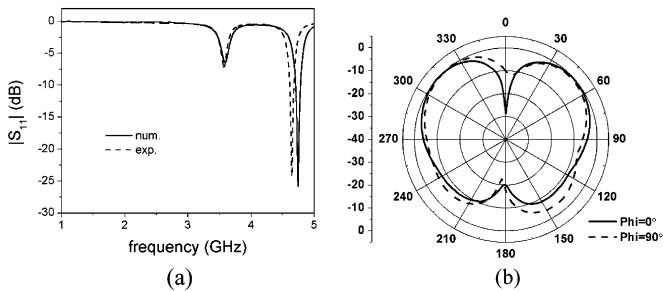
Fig. 20. Enlarged aperture monopolar antenna. (a) Numerical and experimental return loss. (b). Experimental radiation pattern; $\text{phi} = 0°$ (x-z plane), $\text{phi} = 90°$ (y-z plane).

the shift in the infinite frequency is due to the increased mutual coupling attributed to the additional unit-cells. The electrical size of the antennas is $\lambda_o/3 \times \lambda_o/3 \times \lambda_o/53$ at f_0. The experimental radiation patterns at $f_0 = 3.58\,\text{GHz}$ are plotted in Fig. 20(b) and confirm the expected monopolar radiation pattern. A maximum gain of 5.72 dBi is obtained with a more symmetric radiation pattern than the six unit-cell antennas of Section IV-D.

V. CONCLUSION

The design of infinite wavelength resonant antennas based on periodic structures is demonstrated. The frequency of the antenna does not depend on its physical length, but only on the reactance provided by its unit-cell. In particular, the infinite wavelength supported by a CRLH unit-cell and an inductor-loaded unit-cell were used to realize several monopolar antennas. The infinite wavelength frequency is determined by the shunt resonance of the unit-cell. Since the monopolar antenna's physical length is independent of the resonance phenomenon at the infinite wavelength frequency, a monopolar antenna can be arbitrary sized. To demonstrate these concepts, six antennas with different number of unit-cells are numerically and experimentally realized with the CRLH unit-cell and an inductor-loaded unit-cell. Although, the antenna's resonant length is increased by 200%, only a 4.7% frequency shift was obtained for the six unit-cell antenna in comparison to the two unit-cell antenna. These antennas can be used in place of array configurations for increased gain with minimum physical space requirements. In particular, the antenna size/gain can be controlled independently of the antenna's frequency with the proposed infinite wavelength methodology.

REFERENCES

[1] V. G. Veselago, "The electrodynamics of substances with simultaneously negative values of ε and μ," *Soviet Physics Uspekhi*, vol. 10, no. 4, pp. 509–514, Jan. 1968.

[2] R. A. Shelby, D. R. Smith, and S. Schultz, "Experimental verification of a negative index of refraction," *Science*, vol. 292, pp. 77–79, Apr. 2001.

[3] C. Caloz, H. Okabe, T. Iwai, and T. Itoh, "Transmission line approach of left-handed (LH) materials," in *Proc. USNC/URSI National Radio Science Meeting*, San Antonio, TX, Jun. 2002, vol. 1, pp. 39–39.

[4] C. Lee, K. M. K. H. Leong, and T. Itoh, "Design of resonant small antenna using composite right/left-handed transmission line," in *Proc. IEEE Antennas and Propagation Society Int. Symp.*, Jun. 2005.

[5] M. Schüssler, J. Freese, and R. Jakoby, "Design of compact planar antennas using LH-transmission lines," in *Proc. IEEE MTT-S Int. Microwave Symp.*, Jun. 2004, vol. 1, pp. 209–212.

[6] A. Sanada, C. Caloz, and T. Itoh, "Zeroth order resonance in composite right/left-handed transmission line resonators," in *Proc. Asia-Pacific Microwave Confe.*, Seoul, Korea, Nov. 2003, vol. 3, pp. 1588–1592.

[7] A. Lai, K. M. K. H. Leong, and T. Itoh, "A novel N-port series divider using infinite wavelength phenomena," in *IEEE-MTT Int. Symp. Dig.*, Long Beach, CA, Jun. 2005.

[8] A. Sanada, M. Kimura, I. Awai, H. Kubo, C. Caloz, and T. Itoh, "A planar zeroth-order resonator antenna using left-handed transmission line," in *Proc. Eur. Microwave Conf.*, Amsterdam, The Netherlands, Oct. 2004.

[9] C. Delaveaud, P. Leveque, and B. Jecko, "New kind of microstrip antenna: The monopolar wire-patch antenna," *Electron. Lett.*, vol. 30, no. 1, pp. 1–2, Jan. 1994.

[10] J. S. Row, S. H. Yeh, and K. L. Wong, "A wide-band monopolar plate-patch antenna," *IEEE Trans. Antennas Propag.*, vol. 50, no. 9, pp. 1328–1330, Sep. 2002.

[11] K. L. Lau, P. Li, and K. M. Luk, "A monopolar patch antenna with very wide impedance bandwidth," *IEEE Trans. Antennas Propag.*, vol. 53, no. 3, Mar. 2005.

[12] C. Decroze, G. Villemaud, F. Torres, and B. Jecko, "Single feed dual-mode wire patch antenna," in *Proc. IEEE Antennas and Propagation Society Int. Symp.*, Jun. 2002, vol. 1, pp. 22–25.

[13] R. Waterhouse, S. D. Targonski, and D. M. Kokotoff, "Design and performance of small printed antennas," *IEEE Trans. Antenna Propag.*, vol. 46, no. 11, pp. 1629–1633, Nov. 1998.

[14] C. A. Balanis, *Antenna Theory*, 2nd, Ed. New York: Wiley, 1997.

[15] D. Sievenpiper, L. Zhang, F. J. Broas, N. G. Alexopulos, and E. Yablonovitch, "High-impedance electromagnetic surfaces with a forbidden frequency band," *IEEE Trans. Microwave Theory Tech.*, vol. 47, pp. 2059–2074, Nov. 1999.

[16] A. Sanada, C. Caloz, and T. Itoh, "Planar distributed structures with negative refractive properties," *IEEE Trans. Microwave Theory Tech.*, vol. 52, pp. 1252–1263, Apr. 2004.

[17] A. Lai, C. Caloz, and T. Itoh, "Composite right/left-handed transmission line metamaterials," *IEEE Microwave Mag.*, vol. 5, no. 3, pp. 34–50, Sep. 2004.

[18] A. Lai, K. M. K. H. Leong, and T. Itoh, "Dual-mode compact microstrip antenna based on fundamental backward wave," presented at the Asia Pacific Microwave Conference, Suzhou, China, Dec. 2005.

[19] E. Chang, S. A. Long, and W. F. Richards, "An experimental investigation of electrically thick rectangular microstrip antennas," *IEEE Trans. Antennas Propag.*, vol. 34, no. 6, pp. 767–772, Jun. 1986.

[20] N. Mercé, P. Tejedor, and J. Vassal'lo, "The TM_{01} mode of microstrip radiators and some of its applications," in *IEEE Antennas and Propagation Society Int. Symp.*, Apr. 1995, pp. 33–36.

[21] C. Martín-Pascual and I. Seoane, "On the generation and applications of the monopolar ("zeroth" like) mode in non-circular patches," in *Proc. 17th Int. Conf. on Applied Electromagnetics and Communications*, Dubrovnik, Croatia, Oct. 2003, pp. 160–163.

[22] J. S. Dahele, K.-F. Lee, and P.-Y. Lee, "Experimental study of the characteristics of coupled top-loaded microstrip monopoles," *IEEE Trans. Antennas Propag.*, vol. 31, pp. 530–531, May 1983.

[23] J.-S. Row, S.-H. Yeh, and K.-L. Wong, "A wide-band monopolar plate-patch antenna," *IEEE Trans. Antennas Propag.*, vol. 50, no. 9, pp. 1328–1330, Sep. 2002.

[24] D. M. Pozar and B. Kaufaman, "Comparison of three methods for the measurement of printed antenna efficiency," *IEEE Trans. Antennas Propag.*, vol. 36, pp. 136–139, Jan. 1988.

[25] R. E. Collin and F. J. Zucker, *Antenna Theory*. New York: McGraw-Hill, 1969.

Anthony Lai (S'00) received the B.E. degree in electrical engineering from The Cooper Union for the Advancement of Science and Art, New York City, in 2001 and the M.S. degree in electrical engineering from the University of California, Los Angeles (UCLA), in 2005. He is currently working toward the Ph.D. degree in electrical engineering at UCLA. His research interests include metamaterial applications and planar antennas.

Kevin M. K. H. Leong (S'99–M'04) received the B.S. degree in electrical engineering from the University of Hawaii at Manoa in 1999 and the M.S. degree and Ph.D. in electrical engineering from the University of California at Los Angeles, in 2001 and 2004, respectively.

He is currently a Postdoctoral Researcher at UCLA. His research interests include planar antennas, millimeter-wave circuits, and mobile communication systems.

Dr. Leong was the first place winner of the best-student paper contest at the 2001 European Microwave Conference.

Tatsuo Itoh (S'69–M'69–SM'74–F'82) received the Ph.D. degree in electrical engineering from the University of Illinois, Urbana, in 1969.

From September 1966 to April 1976, he was with the Electrical Engineering Department, University of Illinois. From April 1976 to August 1977, he was a Senior Research Engineer in the Radio Physics Laboratory, SRI International, Menlo Park, CA. From August 1977 to June 1978, he was an Associate Professor at the University of Kentucky, Lexington. In July 1978, he joined the faculty at The University of Texas at Austin, where he became a Professor of Electrical Engineering in 1981 and Director of the Electrical Engineering Research Laboratory in 1984. During the summer of 1979, he was a guest researcher at AEG-Telefunken, lm, West Germany. In September 1983, he was selected to hold the Hayden Head Centennial Professorship of Engineering at The University of Texas. In September 1984, he was appointed Associate Chairman for Research and Planning of the Electrical and Computer Engineering Department at The University of Texas. In January 1991, he joined the University of California, Los Angeles as Professor of Electrical Engineering and held the TRW Endowed Chair in Microwave and Millimeter Wave Electronics. He was an Honorary Visiting Professor at Nanjing Institute of Technology, China and at Japan Defense Academy. In April 1994, he was appointed as Adjunct Research Officer for Communications Research Laboratory, Ministry of Post and Telecommunication, Japan. He currently holds a Visiting Professorship at the University of Leeds, U.K. He has 350 journal publications, 650 refereed conference presentations and has written 30 books/book chapters in the area of microwaves, millimeter-waves, antennas and numerical electromagnetics. He generated 65 Ph.D. students.

Dr. Itoh is a member of the Institute of Electronics and Communication Engineers of Japan, and Commissions B and D of USNC/URSI. He received a number of awards including Shida Award from Japanese Ministry of Post and Telecommunications in 1998, Japan Microwave Prize in 1998, IEEE Third Millennium Medal in 2000, and IEEE MTT Distinguished Educator Award in 2000. He was elected to a member of National Academy of Engineering in 2003. He served as the Editor of IEEE TRANSACTIONS ON MICROWAVE THEORY AND TECHNIQUES for 1983–1985. He serves on the Administrative Committee of IEEE Microwave Theory and Techniques Society. He was Vice President of the Microwave Theory and Techniques Society in 1989 and President in 1990. He was the Editor-in-Chief of IEEE MICROWAVE AND GUIDED WAVE LETTERS from 1991 through 1994. He was elected as an Honorary Life Member of MTT Society in 1994. He was the Chairman of USNC/URSI Commission D from 1988 to 1990, and Chairman of Commission D of the International URSI for 1993–1996. He is Chair of Long Range Planning Committee of URSI. He serves on advisory boards and committees of a number of organizations.